MXene based fibre optic Fabry-Perot interferometer for heavy metal detection

Jiaxing Sun[a], Hanlin Jiang[a], Miles Buchanan[a], Rowan Wain[a], Xianfeng Chen*[a]
[a]School of Science and Technology, Nottingham Trent University,
Nottingham NG11 8NS, United Kingdom

ABSTRACT

In this work, we propose a miniature and high-performance MXene-based fibre optic Fabry-Perot interferometer (FPI) for the detection of heavy metal (mercury) in the water. Light from fibre tips (FP cavity) induce interference through partial reflection at interfaces. The systematic investigations have been conducted for the free spectral range against the FP cavity length, the effect of finesse on the surface reflectance of FP cavity surface using thin film gold-coated fibre tips of various thickness in nanometre scales. The FP fibre tip deposited with MXene nanolayer will be developed to detect Hg^{2+} in water by inducing a strong response through the adsorption and reduction of Hg^{2+} to Hg^{+} with MXene nanomaterials. The nanomaterial integrated FPI sensing scheme could be an alternative for food, water quality, and environmental monitoring.

Keywords: Fibre sensor, Fabry-Perot, nano-film, nanomaterial, heavy metal

1. INTRODUCTION

Heavy metal ions are usually toxic and carcinogenic with the harmful effects to the environment, food and water quality, and human health. The World Health Organization (WHO) has listed the mercury as one of the most toxic heavy metals [1], which can be commonly found in the biosphere, atmosphere, and hydrosphere. Due to the release of ~ 2,000 tonnes of mercury into the environment each year from human activities, approximately 1.5 million people worldwide are at risk of developing health problems due to mercury exposure [1]. In water, mercury is usually present as Hg^{2+}, which bioaccumulates and biomagnifies, causing severe neurological effects in humans by binding to mercaptan residues contained in proteins [3]. Therefore, the detection of mercury in water becomes a major public concern in modern days. Various technologies have been developed for detecting Hg^{2+}, such as inductively coupled plasma mass spectrometry, atomic fluorescence spectrometry, atomic absorption spectroscopy, atomic emission spectrometry, fluorescence, and electrochemical approaches [7]. However, the traditional methods require large instruments, complex sample preparation, strict detection conditions, and lack of in-situ detection. Over the last decades, fibre optic sensing technology has been significantly developed and provided many advantages such as immunity to electromagnetic interference, miniaturisation, cost-effectiveness, and rapid detection [8,9]. To date, 2D layered nanomaterials including graphene and its derivatives, black phosphorus, and transition metal carbides/carbonitrides (i.e., MXene) have attracted great excitement due to their extraordinary mechanical, chemical, and optoelectronic properties. It is imperative to investigate novel and portable sensor for rapid heavy metal detection.

2. METHODOLOGY

In this work, we have systematically investigated the properties of fibre optic Fabry-Perot interferometer (FPI). As the schematic diagram of FPI shown in Figure 1, two single mode fibres (SMFs) are inserted into a glass capillary tube, two finely cleaved fibre surfaces are well aligned acting as two parallel reflecting mirrors (M1, M2) to build a FP cavity.
When the light is launched from left side of SMF-1 and passes through the FP cavity, it is multiply reflected by the parallelly paired mirrors where the reflected lights are collected by the SMF-1 back to the optical spectrum analyser (OSA) showing the apparent interference pattern/spectrum.

* xianfeng.chen@ntu.ac.uk

Jiaxing Sun, Hanlin Jiang, Miles Buchanan, Rowan Wain, and Xianfeng Chen "MXene-based fibre optic Fabry-Perot interferometer for heavy metal detection", Proc. SPIE 13083, SPIE Future Sensing Technologies 2024, 1308312 (28 May 2024); https://doi.org/10.1117/12.3023050

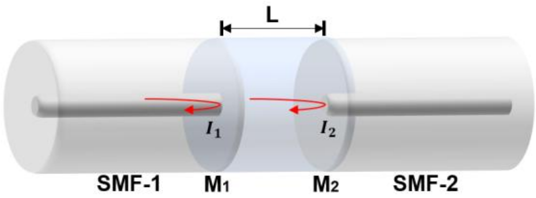

Figure 1. Schematic diagram of fibre optic Fabry-Perot interferometer.

For an FPI, the intensity I_r of the interference spectrum can be expressed as [10]:

$$I_r = I_1 + I_2 + 2\sqrt{I_1 I_2}\, cos\varphi \tag{1}$$

where I_1 and I_2 are the light intensities of two optical beams reflected by M_1, M_2, respectively; φ is the phase difference between two optical beams, which is formulated by:

$$\varphi = \frac{4\pi nL}{\lambda} \tag{2}$$

where L is the FP cavity length, n is the refractive index of the medium in the cavity ($n \approx 1$ when cavity medium is air), λ is the light wavelength. The constructive interference occurs if the reflected beams are in phase, whilst the destructive inference appears when the beams are out-of-phase.

The cavity length L can be calculated from the wavelength of two adjacent resonant dips [11]:

$$L = \frac{\lambda_1 \lambda_2}{2n(\lambda_1 - \lambda_2)} \tag{4}$$

where λ_1, λ_2 are the wavelengths of two consecutive dips in the interference spectrum. The dip's number and wavelength are exclusively dependent on the cavity length and cavity medium.

The wavelength separation $\Delta\lambda$ between adjacent interference peaks is named the free spectral range (FSR), which can be given by:

$$\Delta\lambda = \frac{\lambda^2}{2nL} \tag{4}$$

where λ is the central wavelength of the nearest peak.

For a FP cavity with two mirrors (M1, M2), the finesse $\mathcal{F}$ is defined by [11]:

$$\mathcal{F} = \frac{\pi\, (R_1 R_2)^{\frac{1}{4}}}{1-\sqrt{R_1 R_2}} \tag{5}$$

where R_1, R_2 is the reflectance of M1, M2, respectively. When $R_1 = R_2 = R$, the finesse becomes:

$$\mathcal{F} = \frac{\pi\, \sqrt{R}}{1-R} \tag{6}$$

3. RESULTS AND DISCUSSION

3.1 Free spectral range (FSR) against FP cavity length

To monitor the effect of FSR against the FP cavity length, two mirrors (M1, M2) both with 4% reflectance were used. For a selected spectral observation window (1490-1550 nm, Figure 2a), there were 2, 4 and 6 dips when the cavity length was changed from 40, 80, to 120 μm, respectively. The intensity of interference fringe was reduced when the cavity length was increased as less light energy was reflected by rare mirror (M2) as well as accepted back to the fibre core at M1 due to the divergence of light out of the fibre core. The free spectral range ($\Delta\lambda$) showed a nonlinear effect against the cavity length (Figure 2b), the longer the cavity the smaller the FSR. For example, the FSR decreased from 30.06 to 9.85 then 5.87 nm when the cavity length increased from 40 to 120 then 200 μm, respectively (blue symbols in Fig. 2b).

Jiaxing Sun, Hanlin Jiang, Miles Buchanan, Rowan Wain, and Xianfeng Chen "MXene-based fibre optic Fabry-Perot interferometer for heavy metal detection", Proc. SPIE 13083, SPIE Future Sensing Technologies 2024, 1308312 (28 May 2024); https://doi.org/10.1117/12.3023050

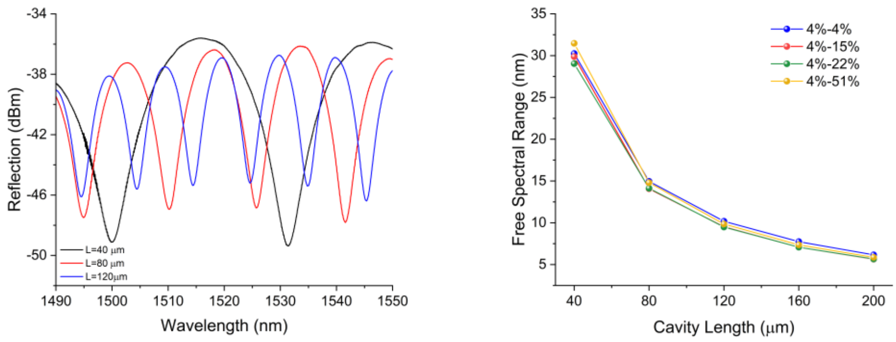

(a) (b)

Figure 2. (a) Interference spectra of FPI for three different cavity lengths. (b) FSR change against cavity length.

The effect of the reflectance of pair of FP mirrors on FSR was investigated as well. The FP cavity consisted of two mirrors (M1, M2), M1 was kept with 4% reflectance (bare fibre end) whilst M2 were coated by gold thin-film with various reflectance values, such as 4% (bare fibre), 15%, 22%, and 51%.

It can be seen from Fig.2b that the FSRs for all four-paired mirrors (4%-4%, 4%-15%, 4%-22%, 4%-51%) show the same nonlinear relationship with the FP cavity length, giving the rates ($\Delta\lambda/\Delta L$) of 0.37 nm/µm, 0.12 nm/µm, and 0.06 nm/µm for short, middle and long cavity length, respectively. The experimental results confirmed that the free spectral range (FSR) can only be affected by the cavity length, not the mirror reflectance (if keep the same medium within the cavity, i.e., the same n), which was expected by the Equation (4).

3.2 Performance of finesse

The finesse ($\mathcal{F}$) of four FPIs with four-paired mirrors (M1-M2) were investigated. Based on Equation (5), the finesse was calculated as 0.65, 0.95, 1.07 and 1.38 for four-paired mirrors of 4%-4%, 4%-15%, 4%-22% and 4%-51%, respectively.

Finesse of the FPI was experimentally characterised by using a broadband light source and an optical spectrum analyser. As shown in Figure 3, for a fixed cavity length (L= 40 µm), the intensity of the interference fringe was 0.28, 0.38, 0.60, and 0.76 µW for the pair of 4%-4%, 4%-15%, 4%-22%, and 4%-51%, respectively, indicating that the finesse was enhanced when the mirror reflectance increased.

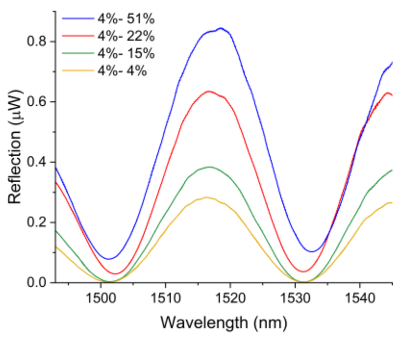

Figure 3. The finesse $\mathcal{F}$ of four FPIs with four-paired mirrors (M1-M2).

An FPI has a high Q factor when it has high finesse. As defined by Equation 5, the sharpness of the interference patterns depends on the reflectance of paired mirrors. The experimental results (Figure 3) show that the spectrum has sharper interference peaks when the reflectance of M2 increases (with high finesse). There are some slight discrepancies between four-paired results, which might be caused by the lateral offset and angular deviation of the paired fibre tips (mirrors).

Jiaxing Sun, Hanlin Jiang, Miles Buchanan, Rowan Wain, and Xianfeng Chen "MXene-based fibre optic Fabry-Perot interferometer for heavy metal detection", Proc. SPIE 13083, SPIE Future Sensing Technologies 2024, 1308312 (28 May 2024); https://doi.org/10.1117/12.3023050

3.3 Hybrid FP-FBG sensor for temperature measurement

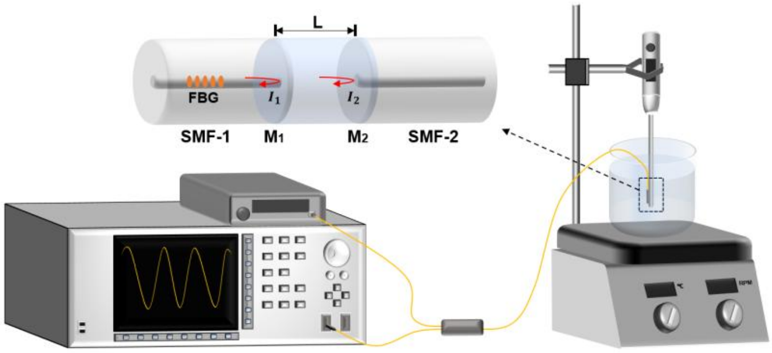

Figure 4. Experimental setup for temperature measurement with a hybrid FP/FBG sensor.

A hybrid FP/fibre Bragg grating (FBG) sensor was proposed (Figure 4), where the FP cavity was built by two fibre tips (4%-4%) inserted into a glass capillary tube with a cavity length of 73 µm whilst a FBG was fabricated with the Bragg wavelength at 1509.91 nm (Figure 5).

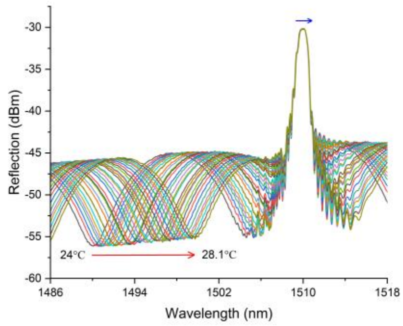

Figure 5. Spectra of hybrid FP/FBG sensor under different temperatures.

The hybrid sensor head was placed into the water heated by a hot plate. When the temperature increased, both FP spectral dips and FBG peak moved to the long wavelength side. As shown in Figure 6, both the FP interferometric wavelength and Bragg wavelength show the linear relationships with the temperature, giving a sensitivity of 2.46 nm/°C and 9.5 pm/°C for FP and FBG, respectively.

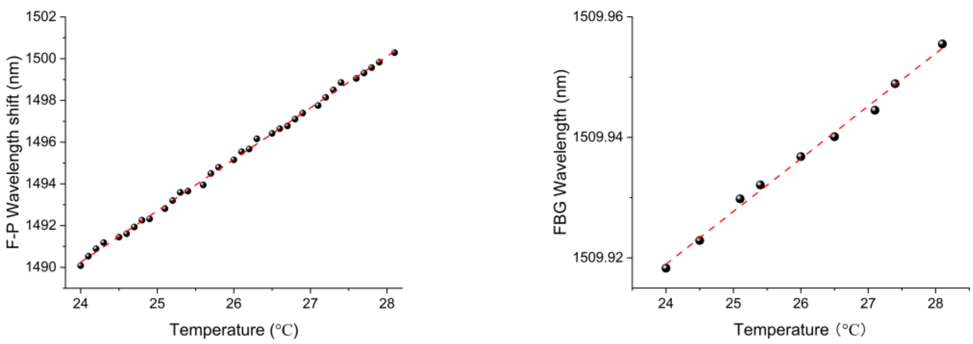

(a) (b)

Figure 6. The wavelength shifts of the (a) FP and (b) FBG against temperature change.

Jiaxing Sun, Hanlin Jiang, Miles Buchanan, Rowan Wain, and Xianfeng Chen "MXene-based fibre optic Fabry-Perot interferometer for heavy metal detection", Proc. SPIE 13083, SPIE Future Sensing Technologies 2024, 1308312 (28 May 2024); https://doi.org/10.1117/12.3023050

4. CONCLUSION

We proposed and experimentally demonstrated a hybrid FPI/FBG sensor. The systematic investigations were conducted for the free spectral range and finesse of FP. Both FP and FBG showed linear relationships for the temperature measurements with sensitivity of 2.46 nm/°C and 9.5 pm/°C, respectively. In future, the FPI fibre tips will be deposited with MXene nanolayer to detect Hg^{2+} in water by inducing a strong response through the adsorption and reduction of Hg^{2+} to Hg^{+} with MXene nanomaterials, where the FBG can be used for temperature compensation. The hybrid fibre optic configuration owns advantages of miniaturisation, portability, high sensitivity and real-time detection for food, water quality, and environment.

ACKNOWLEDGEMENTS

This work has received funding from the European Union's Horizon 2020 research and innovation programme under the Marie Skłodowska-Curie grant agreement No 872049.

REFERENCES

[1] World Health Organization, Guidelines for Drinking-water Quality, 4th ed., 2011.

[2] Liu, J., Shi, J., Zhong, M., Wang, Y., Zhang, X., Wang, W., Chen, Z., Tan, Y., Xu, D., Yang, S. and Li, L. "A novel electrochemical sensing method based on an amino-functionalized MXene for the rapid and selective detection of Hg^{2+}," Analytical Methods 16.2: 244-252 (2024).

[3] Poste, A.E., Pastukhov, M.V., Braaten, H.F.V., Ozersky, T. and Moore, M. "Past and present mercury accumulation in the Lake Baikal seal: Temporal trends, effects of life history, and toxicological implications," Environmental toxicology and chemistry 37.5: 1476-1486 (2018).

[4] Narukawa, T., Iwai, T. and Chiba, K. "Simultaneous speciation analysis of inorganic arsenic and methylmercury in edible oil by high-performance liquid chromatography–inductively coupled plasma mass spectrometry," Talanta 210: 120646 (2020).

[5] Liu, J.L., Han, Q., Hu, E.Y., Yang, C. and Yin, M.M. "Determination of trace mercury in water samples by cloud point extraction coupled with atomic fluorescence spectrometry, Journal of Analytical Chemistry 78.3: 303-309 (2023).

[6] Omeje, K.O., Ezema, B.O., Okonkwo, F., Onyishi, N.C., Ozioko, J., Rasaq, W.A., Sardo, G. and Okpala, C.O.R. "Quantification of heavy metals and pesticide residues in widely consumed Nigerian food crops using atomic absorption spectroscopy (AAS) and gas chromatography (GC)," Toxins, 13(12): 870, (2021).

[7] Guo, Y., Zhang, L., Zhang, S., Yang, Y., Chen, X. and Zhang, M. "Fluorescent carbon nanoparticles for the fluorescent detection of metal ions." Biosensors and Bioelectronics 63: 61-71 (2015).

[8] X. Chen, C. Liu, M. D. Hughes, D. A. Nagel, A. Hine, L. Zhang, "EDC-mediated oligonucleotide immobilization on a long period grating optical biosensor," Journal of Biosensors and Bioelectronics 6 (2), 1000173 (2015).

[9] C. Liu, Q. Cai, B. Xu, W. Zhu, L. Zhang, J. Zhao, X. Chen, "Graphene oxide functionalized long period grating for ultrasensitive label-free immunosensing," Biosens. Bioelectron. 94, 200–206 (2017).

[10] Zhang, Z., Gong, H., Yu, C., Ni, K. and Zhao, C. "Fiber optic Fabry–Perot interferometer based on HA/PVA composite film for humidity sensing. Optical Fiber Technology," 68, p.102816 (2022).

[11] Domínguez-Flores, C.E., Monzón-Hernández, D., Moreno-Basulto, J.I., Rodríguez-Quiroz, O., Minkovich, V.P., López-Cortés, D. and Hernández-Romano, I. "Real-time temperature sensor based on in-fiber Fabry–Perot interferometer embedded in a resin," Journal of Lightwave Technology, 37(4), pp.1084-1090 (2018).

[12] Ghildiyal, S., Balasubramaniam, R. and John, J. "Effect of flatness and parallelism errors on fiber optic Fabry Perot Interferometer of low to moderate finesse and its experimental validation," Optical Fiber Technology, 60, p.102372 (2020).

Jiaxing Sun, Hanlin Jiang, Miles Buchanan, Rowan Wain, and Xianfeng Chen "MXene-based fibre optic Fabry-Perot interferometer for heavy metal detection", Proc. SPIE 13083, SPIE Future Sensing Technologies 2024, 1308312 (28 May 2024); https://doi.org/10.1117/12.3023050